Chapter 5
Reengineering the Connectome with Photon Assisted Synaptic Transmission (PhAST)

Michael Krieg

Abstract The emergence of comprehensive connectomes in organisms, like *Caenorhabditis elegans*, Drosophila, and the mouse, is transforming our understanding of neural circuit architecture. Manipulating these circuits noninvasively, however, remains a major challenge. Optogenetics is a promising neuromodulation technique but requires external light to activate neurons within the target tissue. To address this, we recently developed and deployed photon-assisted synaptic transmission, or short PhAST, a system of bioluminescence-driven optogenetics, where light is generated directly within presynaptic neuronal compartments through luciferase-luciferin reactions and activates postsynaptically expressed channelrhodopsins. Using the PhAST strategy in *C. elegans*, we demonstrated activity-dependent, transsynaptic activation of channelrhodopsins to restore disrupted signaling without external light. Photon emission from luciferases, broadly distributed along axons and gated by intracellular messengers such as calcium, enables flexible, synapse-independent information transfer, even under conditions of vesicular transmission failure. This modular system not only bypasses the physical limitations of traditional optogenetics but also sets the stage for programmable, stimulus-responsive networks that leverage intrinsic signaling dynamics for precision neuromodulation.

Keywords Bioluminescence · Connectome engineering · Optogenetics · Neuromodulation · Synaptic transmission

M. Krieg (✉)
ICFO – Institut de Ciències Fotòniques, Castelldefels, Spain

The Barcelona Institute of Science and Technology, Barcelona, Spain
e-mail: michael.krieg@icfo.eu

U. Hochgeschwender (ed.), *BioLuminescent OptoGenetics*,
https://doi.org/10.1007/978-3-032-18121-3_5

5.1 Introduction

Fueled by recent breakthroughs in large-scale connectome reconstructions from multiple species, unprecedented opportunities arise for understanding and manipulating brain functions [1–4]. Several strategies have been introduced in recent years that allow researchers to modulate neuronal activity through chemical, electric, magnetic, acoustic, and optical stimulation [5]. Whereas the first four methods leverage the endogenous sensitivity of the central nervous system to these stimuli, optical neuromodulation, commonly referred to as optogenetics, requires the neuronal expression of a dedicated light sensor.

This is commonly achieved using microbial channelrhodopsins, special ion channels which respond to blue, green, or orange light, and selectively conduct ions to depolarize or hyperpolarize the neuronal membrane potential [6]. Due to the poor light sensitivity of these channels, together with the high scattering properties of healthy brain tissue, optogenetics in the mammalian brain requires the implantation of a light diode [7]. However, this also confers exceptional precision, enabling control at the level of individual cell types—or even specific synapses [8]. The following table summarizes the pros and cons of four different neuromodulation techniques (Table 5.1).

5.2 Principle of PhAST

Considering that the risks of gene transfer are acceptable in severe health conditions, several strategies are currently discussed to improve light delivery to channelrhodopsins. Among those are red-shifted channelrhodopsins, such as ChRmine [9] and ChReef [10] and rhodopsins, with an extended open-state lifetime that confers an exceptional operational light sensitivity [11]. Although the mentioned options minimize invasiveness, depending on the location of the target neurons within the brain, they may require high intensities that could cause tissue damage due to heating and generate reactive oxygen species. To minimize energy

Table 5.1 Compact comparison of neural stimulation modalities

Modality	Advantages	Disadvantages
Chemical	Activates endogenous receptors	Slow; low spatial precision; off-target effects
Electrical	Clinically established; fast and reversible	Low spatial resolution; invasive; tissue damage
Magnetic	Noninvasive; deep penetration; clinically safe	Low precision; indirect; hard to focus
Acoustic	Noninvasive; deep targets w/focused ultrasound	Mechanism unclear; potential damage; calibration needed
Optical	Cell-type precision; high spatial/temporal resolution	Requires gene delivery and optrode implantation; phototoxic

deposition, an alternative approach is to generate light noninvasively within the target tissue, either through bioluminescence [12] or via luminescent nanoparticles with tunable and controlled emission [13–15].

As described extensively throughout this book, bioluminescence is a form of chemiluminescence mediated by biological systems, in which the enzymatic oxidation of a 'luciferin' by a luciferase leads to the formation of an electronically excited product that decays to the ground state via photon emission, typically in the 400–700 nm wavelength range [12]. Because this process requires additional substrates and cofactors, the light emission can be coupled to the presence of Ca^{2+}, ATP, and oxygen (see also Table 5.2). Furthermore, luciferases can be engineered to emit a photon only in the presence of high calcium concentrations that are typical for activated neurons [16, 17], for example, those that occur during synaptic transmission. These enzymes have been recognized as ideal calcium-dependent light switches that can be functionally coupled to channelrhodopsins [18] (Fig. 5.1) expressed in the same cell or on the postsynaptic compartment of the synapse between two neurons.

Table 5.2 Selection of bioluminescent sensors used for intracellular metabolite detection that are of interest for synaptic engineering purposes, including their target molecules, optical systems, key features, and reference

Sensor name	Target metabolite	Luciferase	Key features	Ref.
Nanolantern	Ca^{2+}	Renilla Luc BRET with FP	Low photon output	[21]
Enhanced Nanolantern	Ca^{2+}	Split NanoLuc with CaM/M13 and FP	High sensitivity; live-cell imaging	[16, 22]
GLICO	Ca^{2+}	NanoLuc	2200% dynamic range; GCaMP6f	[23]
ReBLICO	Ca^{2+}	NanoLuc	Low affinity for ER imaging	[23]
LUCI-GECO1	Ca^{2+}	NanoLuc	GCaMP6s; ratiometric	[24]
BRIC	Ca^{2+}	teLuc		[25]
CaBLAM	Ca^{2+}	eKaz	15- to 20-fold change in cells	[26]
CaMBI3	Ca^{2+}	NanoLuc	Antares-based, 580 nm peak emission	[27]
BLING1.0	Glutamate	NanoLuc	Glt1 glutamate binding protein and PDGFRβ transmembrane anchor	[28]
LuCID	Ca^{2+}	Split NanoLuc + Gal4	Slow response; Coupled to gene expression	[29]
BTeam	ATP	NanoLuc BRET with YFP	High sensitivity; live- cell imaging	[30]
Nanolantern (cAMP1.6)	ATP	Renilla	Fused to fragment of EPAC1, 1.6 μM affinity	[21]
iNap-BL	NADPH	Lux operon	Tracks NADPH; high S/N ratio	[31]
LOTUS-Glc	Glucose	NanoLuc	MglB domain, ratio metric	[32]

For a more detailed compendium, refer to [33]

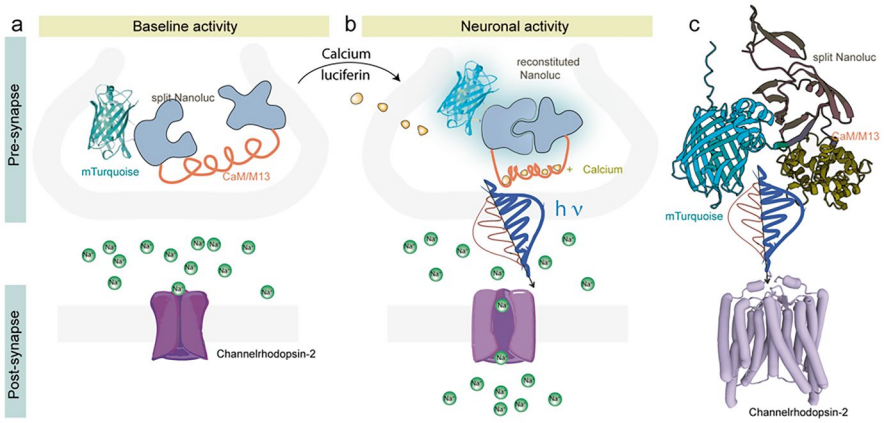

Fig. 5.1 Schematic of the PhAST principle based on split-enhanced Nanolantern and channelrhodopsin. (**a**) Under conditions of low baseline neuronal activity—and consequently low calcium levels in the presynaptic neuron—photon output is insufficient to trigger transsynaptic activation of channelrhodopsins. (**b**) High presynaptic neuronal activity, accompanied by a natural calcium influx, leads to the reconstitution of split luciferase enzymatic activity. The resulting increased quantum yield drives activation of the postsynaptic channelrhodopsin, leading to the postsynaptic depolarization and eventually signal transmission. Note, luciferases and channelrhodopsin do not require synaptic specialization but can also drive functional connections along axon-axon fascicles. (**c**) AlphaFold2 models of the presynaptic TeNL [19] and the postsynaptic channelrhodopsin (lilac)

PhAST, in contrast to interluminescence, which required the luciferase to diffuse across the synaptic cleft and get into a FRETting distance with the light receptor, activates the receptor through emission/reabsorption of the photons. Because the synaptic cleft (20–50 nm) is much lower than the wavelength of the emitted light (450 nm), photons are not scattered, and losses due to absorption are avoided. To demonstrate PhAST's versatility, the strategy was extended to multiple circuits in *C. elegans* to overcome transmission defects and to engineer ectopic, de novo connections between naturally unwired neurons. For example, transsynaptic activation of a photosensitive channelrhodopsin was demonstrated in *C. elegans*, leveraging its well-mapped connectome and the previously characterized nocifensive nose touch circuit [20]. This circuit consists of a pair of glutamatergic sensory neurons, called ASH, which synapse onto various interneurons, including AVA and AIB, which in turn instruct the motor circuit (Fig. 5.2a). In 75% of the cases, activation of ASH due to a mechanical stimulus causes a reversal response. In this system, photon emission was precisely controlled using a presynaptic, calcium-sensitive enhanced mTurquoise Nanolantern (TeNL) to restore functional connectivity in a glutamate-deficient mutant. This mutant lacked transmission between the ASH sensory neuron and its downstream interneurons, AVA and AIB [18] (Fig. 5.2).

Intriguingly, because luciferases are broadly distributed across the entire length of the neuron (unless they are specifically targeted to synapses using synaptogyrin tags [18]), PhAST does not require synaptic specializations for information transfer.

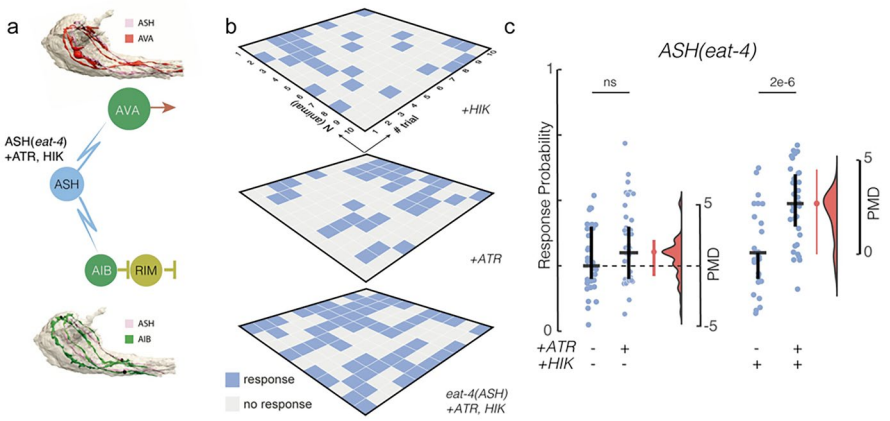

Fig. 5.2 Prosthetic, light-based neurotransmission replaces chemical neurotransmitter. Panel (**a**) is a flow chart illustrating neural pathways involving ASH lacking glutamate transmission (ASH:eat-4 mutant), AVA, AIB, and RIM neurons, with edges indicating synaptic connections colored by their neurotransmitter used. Upon reconstitution with all-trans retinal (ATR) and hikarazine (HIK), the functional, light-based connection is established (blue flashes). Blue flash, photons; red arrow, acetylcholine; yellow arrow, glutamate as neurotransmitter. (**b**) Representative outcome of a single experiment displayed as a raster diagram of the nose touch behavior experiment of the ASH-specific *eat-4* mutant in the presence of the necessary cofactors (Hik, ATR). Ten animals have been touched ten times successively, and each positive response is recorded as a blue square. (**c**) Summary of the average behavioral response of each animal for the different tested conditions presented a scatter plot with response probability on the y-axis and different conditions on the x-axis, showing data points, median values (±95% confidence interval), and statistical significance markers (ns and 2e-6). The floating axis indicates the paired median difference (PMD) between the two conditions to the left of it

This affords signaling even if vesicular release is deficient but may have the downside that signaling happens anywhere along the axon. A transient photon release anywhere in the axons can potentially activate neighboring channelrhodopsin-expressing neurons in an "en passant" synapse-like manner. This may also be harnessed for backpropagation, e.g., ascending information transfer from the postsynaptic (dendrite) to the presynaptic (axon) neurons.

Because light emission can also be coupled to other secondary messengers of cellular signaling cascades, such as ATP and cAMP (see Table 5.2), this principle is universal and affords the design of new-to-nature stimulus-responsive neuronal networks.

5.3 Requirements for Successful Photo-transmission

In the following sections, we will discuss the three main components of a light-based synapse, which consists of a light emitter, a light sensor, and luciferin, which is the actual chromophore required for photon emission.

5.3.1 Luciferases

Because luciferases in general have a duty cycle slower than that of fluorescent proteins and therefore have a lower photon budget, the most powerful luciferases are needed for PhAST. As mentioned above, the control of their light emission should be tight, meaning that the exposure to the cofactor is transient and the emission is of flash-type to avoid prolonged ChR2 activity without baseline activity.

Alternatively, if the cofactor is constitutively present, light emission may be coupled to a secondary messenger, such as ATP, calcium ions, or glucose concentration. Table 5.2 already exemplifies the current version of genetically encoded sensors of various metabolites that are poised to be deployed in synthetic circuits, together with their color-matched channelrhodopsin. To link pairs or cohorts of neurons based on presynaptic activity, reconstituting light emission in a split luciferase with a calcium-sensitive domain provided a useful platform for functional PhAST signaling [18]. The calcium dependence of the luciferase ensures that light emission is synchronized with neuronal activity, thereby conserving substrate and avoiding issues associated with constitutively active luciferases, such as substrate depletion [34] and enzyme inactivation from rapid catalysis [35]. A high dynamic range and high absolute photon numbers are desired parameters. If combined with slow-closing channelrhodopsins, on/off kinetics may be of secondary choice. For PhAST, enhanced calcium-sensitive Nanolanterns with a Kd = 250 nM of the calcium sensor have been successfully used, but the newer version promises to enter the field [26]. Brighter luciferases could enable the use of faster channels, thereby preserving the rapid dynamics of synaptic signaling, reflecting the inherent change in neuronal circuit dynamics.

5.3.2 Luciferins and Cofactors

All luciferases require a chemical substrate, a so-called luciferin, that is enzymatically oxidized. Chemical structures of luciferins differ depending on the luciferase used. In the experiments reported below, we utilize luciferins optimized for NanoLuc, such as fluorofurimazine (FFz) and Hikarazine (HIK). The luciferase-luciferin reaction requires oxygen, and sometimes a cellular metabolite as a secondary cofactor. This metabolite could be ATP, cAMP, NADH, calcium, or other more

exotic molecules [36] that are already present in the cell. In heterologous systems, the luciferin, in contrast, needs to be added externally. This has advantages and disadvantages depending on the desired outcome. The advantage is that the background activity of the transgenic circuit expressing the luciferase and the channelrhodopsin can be determined in the absence of the light emission without the cofactor. The addition of luciferin, hence, initiates light emission, which provides a direct evaluation of the photon emission to bridge synaptic defects. The disadvantage of this approach is that the bioavailability of many luciferins, especially those used by marine luciferases, may be a limiting factor [12]. Therefore, special media formulations that improve solubility and tissue transport and high concentrations may be required.

5.3.3 Channelrhodopsins

For PhAST, the postsynaptic light sensor is typically an ion channel that coordinates a light-sensitive group, most commonly the vitamin A derivative all-trans retinal (ATR). *C. elegans*, different from mammals, does not produce ATR itself, and thus ATR has to be added as a cofactor. When channelrhodopsins (ChRs) absorb light, the light-sensitive group changes shape from an all-trans form to a 13-cis form, which is coupled to conformational changes in the protein that render it more conductive for a specific ionic species. This shape change starts a series of steps that eventually return the molecule to its original state—this full process is called the photochemical reaction cycle. Compared to typical ion channels, ChRs conduct much smaller amounts of current. Their single-channel conductance is only tens to hundreds of femtoSiemens (fS), while most regular ion channels have conductances in the range of 5 to 500 picoSiemens (pS, see also Table 5.3). Because of this, ChRs behave more like transporters than typical fast ion channels and are lousy neuronal actuators. Combined with the poor quantum yield of the luciferases, this is a deadly combination. Luckily, the low conductance can be offset by longer open state lifetimes, which extends time the channel resides in the ion-conducting conformation, effectively increasing the operational light sensitivity. This does not mean that the ion channel is more sensitive, but the charge transported per photon absorption is higher. Thus, even in photon-starved conditions and a low probability of activation, significant current can be produced [11]. Several naturally occurring and synthetic light-gated ion channels are known to conduct a specific ionic species, for example, H^+, Na^+, Ca^{2+}, K^+, or Cl^-. The former three depolarize neuronal membrane potential and can be used to activate neuronal signaling, whereas the latter two commonly hyperpolarize and therefore suppress neuronal activity. In contrast to presynaptic channelrhodopsins, where a high calcium conductance more effectively triggers synaptic release, postsynaptic channelrhodopsins should favor fast sodium channels to induce rapid spiking and prevent calcium-mediated adaptation mechanisms.

Table 5.3 Different channelrhodopsins and their properties

Variant	Peak abs. (nm)	Conductance	Primary ion selectivity	^{r}*open*	Ref.
ChR2 (WT)	~470	40–70 fS	Nonselective cation (Na^+, H^+)	~13.5 ms	[37]
ChR2-H134R	~470	Increased vs. WT	Na^+	~17.9 ms	[38]
ChR2-XXL (D156C)	~480	750 fS	Nonselective cation	≈70 s	[39]
ChR2-HRDC (H134R+D156C)	~480	?	Nonselective cation	Tens of seconds	[18, 40]
SSFO (C128S, D156A, T159C)	488	?	Na^+	30 min	[11]
Kalium ChR (HcKCR1)	540–550	700 pS	K^+-selective	≈25 ms	[41]
HcKCR1-C110A	540–550	Not specified	K^+-selective	≈25 ms	[42]
ChRmine	~530	110 fS	Na^+-selective	>300 ms	[10, 43]
ChReef	~530	110 fS	Na^+-selective		[10]
GtACR1	515	1.2 pS	Anion (Cl^-)	Fast (~5–10 ms)	[44]
GtACR2	470	0.7 pS	Anion (Cl^-)	Fast (<10 ms)	[44]

ChR2 channelrhodopsin, *ChReef* channelrhodopsin that excites efficiently, *GtACR Guillardia* theta anion channelrhodopsins, *HcKCR Hyphochytrium catenoides* potassium channelrhodopsin

5.3.4 Source-Sink Distance

Contrary to volumetric neurotransmission, which by definition is long-lasting and long-range, PhAST requires close contacts between the photon-emitting cell and the photosensitized receiver cells. Even though we have not formally established the maximum distance between two neurons at which PhAST can still successfully initiate signaling, we performed simulations that model photon propagation through biological tissues. These results suggest a steep drop in signal intensity due to absorption and scattering, and most notably due to geometric dilution (because as the light travels outward, it spreads over the surface of a growing sphere centered at the source). In *C. elegans*, which does not have hemoglobin, the intensity drops by a factor of 10^4 over a few hundred μm [18], while this factor is likely much larger in the mammalian brain [45].

Our subsequent experiments further suggest that synaptic specializations are not required, as two neighboring cells expressing PhAST can influence each other. This is an asset when the activity state shall be transferred onto an anatomically unconnected neuron but may cause unwanted cross talk if multiple neurons express PhAST components.

5.4 Excitatory Synaptic Transmission

Repairing 'broken' circuits PhAST has been successfully implemented in *C. elegans* to restore synaptic transmission deficits both between multiple neurons and at the neuromuscular junction. In both cases, the system was used to restore effective signaling: first, by compensating for a glutamatergic transmission defect between defined neurons and, second, by overcoming synaptic silencing induced by tetanus toxin expression in neurons presynaptic to egg-laying muscles. In both cases, presynaptic emission of the mTurquoise-coupled Nanoluciferase (TeNL) light emission from the presynaptic neuron was used to trigger postsynaptic channelrhodopsin activity. In the first case, neuronal activity in the mechanosensory ASH neuron was triggered by a mechanical stimulus delivered to the nose of the animal, either by an obstacle, which induced a behavioral avoidance response, or in a microfluidic device, in which the activity of the postsynaptic neuron can be followed by calcium imaging as an indicator of neurotransmission. In successful cases, the calcium increase on the postsynaptic neuron was correlated with a behavioral change of the animals, directly demonstrating that photons can act as synaptic neurotransmitters in vivo.

Engineering a gain-of-function Intriguingly, this ectopic photon-based pathway can not only rescue a transmission defect but also be used to engineer a gain-of-function within the same circuit and sensitize naturally insensitive animals to external mechanical stimuli. For example, in the nose touch circuit, no synapses between ASH and AVA have been found in the male connectome [1], and males are less sensitive to chemical [46] and mechanical stimuli (Fig. 5.3a and Ref. [18]). Indeed, AVA in males did not show elevated Ca^{2+} levels in response to mechanical stimulation via the Trap'N'Slap device (Fig. 5.3b), while AIB responded, even though to a lesser degree than hermaphrodites. Behavioral tests confirmed this sexual dimorphism: While males still avoided the stimulus when touched on the nose, their responses were significantly reduced compared to hermaphrodites (Fig. 5.3c).

To enhance this male sensitivity to nose touch, we expressed PhAST in ASH, AVA, and AIB and performed both mechanical (Fig. 5.3c) and optical avoidance assays [18]. With both cofactors (the luciferin Hikarazine, HIK, and the ChR chromophore all-trans retinal, ATR) present, males responded nearly indistinguishably from hermaphrodites, demonstrating that ectopic connections can sensitize neurons and create new behaviors (Fig. 5.3c).

PhAST at the excitatory neuromuscular junction In the second application, PhAST reinstated excitatory transmission at the neuromuscular junction after synaptic vesicle release was selectively inhibited in motoneurons by tetanus toxin (TeTx) expression. We used the egg-laying circuit of *C. elegans* as a model circuit for NMJ function [47], in which VC motorneurons and the hermaphrodite specific neurons HSN form synaptic contacts with the vulval muscles, vm2 (Fig. 5.4a and Ref. [48]). Under normal conditions, the VC and HSN motor neurons cooperatively induce calcium transients in the vulval muscles (vm), (Fig. 5.4a ii, and Ref. [18]). The expression of tetanus toxin (TeTx) in HSN, VC, or both neurons significantly

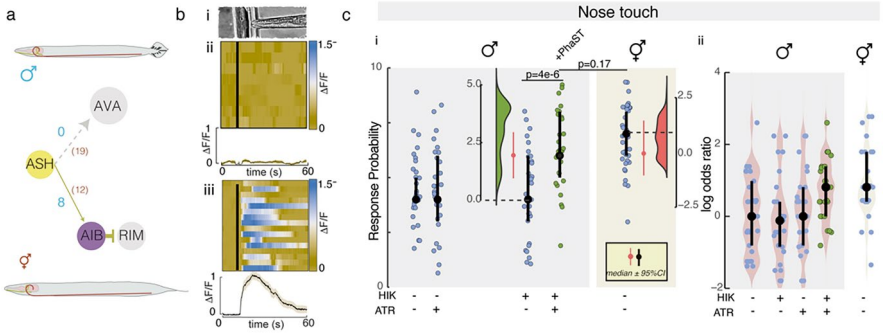

Fig. 5.3 PhAST confers gain-of-function to nociception in a dimorphic circuit. (**a**) Sexually dimorphic connectivity of the ASH nociceptive avoidance circuit, with the number of connections between ASH and AVA or AIB observed in males (blue numbers) or the ones from hermaphrodites (brown font). (**b**) (*i*) Image of an animal inside the Trap'N'Slap device. Stacked kymographs of multiple neuronal calcium recordings from AVA after direct mechanical stimulation of ASH in a microfluidic device. (ii) Response for male animals, (iii) shows the response in hermaphrodites. Blue indicates high neuronal activity; brown indicates baseline activity. Graph below the kymograph indicates the average calcium response of all recordings in the kymograph. Reproduced with permission from [18]. (**c**) Outcome of the nose touch experiment. (*i*) Response probability of male animals expressing the PhAST system in the presence and absence of the ATR and Hikarazine (HIK) cofactors, compared to untreated hermaphrodites of the same genotype ($N = 30$ animals). Moss green data points = functional PhAST after cofactor delivery. Floating axis represents the paired mean difference between control males and PhAST males (green histogram to the left), and between PhAST males (moss green) and control hermaphrodites (red histogram to the right). (*ii*) Violin plots of the log-odds ratio of detecting a positive response in the indicated animals compared to untreated control males (leftmost violin). Moss green data points = functional PhAST after cofactor delivery. Rightmost column indicates the log-odds ratio for detecting a positive response of hermaphrodite control animals compared to untreated males. Filled circle indicates the median; vertical bar indicates 95% CI of the median

reduced spontaneous vm calcium activity (Fig. 5.4b). Notably, this reduction could not be rescued by PhAST when both neurons lacked endogenous transmission, regardless of whether PhAST was expressed in HSN, VC, or both (Fig. 5.4d and Ref. [18]).

However, when VC transmission remained intact, PhAST-mediated restoration of HSN activity successfully rescued vm calcium transients (Fig. 5.4c and Ref. [18]). These complex and seemingly counterintuitive results align with a recently proposed disinhibitory circuit, where VC activity suppresses the inhibitory influence of the neuroendocrine uv1 cells on HSN. In this model, loss of VC neurotransmission leads to sustained uv1 activity, which tonically suppresses HSN excitability and functionally silences its contribution to vulval muscle (vm) activation, even if HSN retains the intrinsic ability of producing depolarizing output.

Our findings, supported by a kinetic model that incorporates this disinhibitory interaction (Fig. 5.4a-d *iv* and Ref. [18]), underscore both the therapeutic potential of synaptic engineering and its utility to uncover functional connectivity in poorly characterized neuronal circuits.

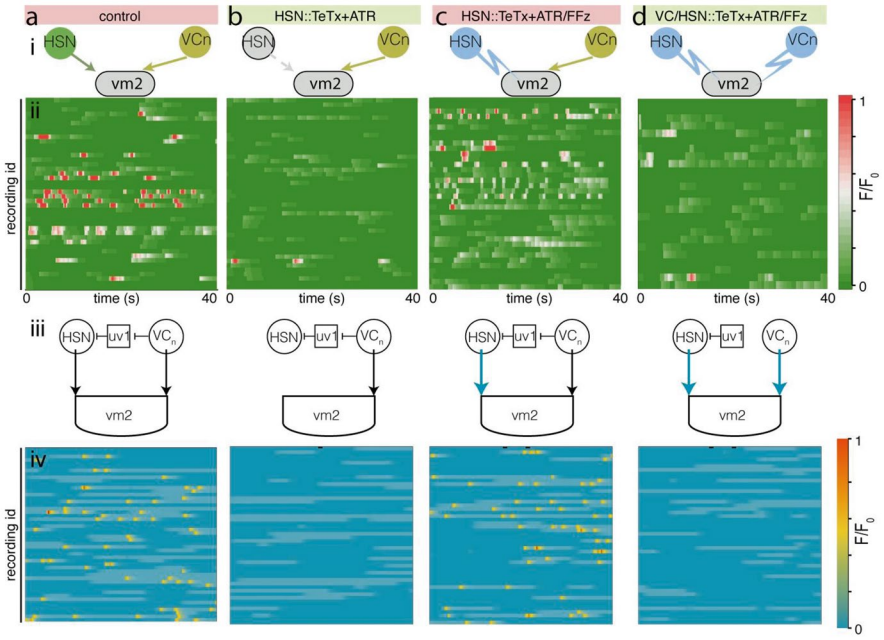

Fig. 5.4 PhAST at the neuromuscular junction. PhAST can be used to dissect the wiring pattern of an unknown neuronal circuit by stepwise expression and activation of photon emission in the individual parts. For all panels: (*i*) Schematics of the egg-laying circuit. Nodes are color-coded by the neurotransmitter used; edges indicate functional connection using chemicals (arrows) or photons (flashes). Green, serotonin; yellow, acetylcholine; blue, photons. (*ii*) Kymographs showing spontaneous calcium activity in vm2 from PhAST animals supplemented with ATR and the luciferin fluorofurimazine, FFz. Color scale indicates the normalized neuronal activity. (*iii*) Schematic of the simulated egg-laying circuit incorporating a possible disinhibitory edge connecting VC and HSN through the neuroendocrine cells uv1. HSN and VC are connected by an AND gate to the vm2 calcium activity. Only if both neurons are "on" and provide input, vm2 responds with an increase in activity. Black edges are normal, wild-type connections; missing edges represent mutant conditions (or tetanus toxin (TeTx) expression), and blue edges represent PhAST connections. (*iv*) Stacked kymographs of the outcome of the simulation of the vm activity, considering the circuit pattern shown above. Yellow indicates high; blue indicates low activity. Data taken and replotted from [18]. **a** vm2 activty in unperturbed control animals. (**b**) vm2 activity in animals expressing TeTx in HSN to interfere with presynaptic signaling. (**c**) Outcome of functional PhAST in HSN on vm2 activity in animals expressing TeTx in HSN to interfere with presynaptic signaling. (**d**) Outcome of functional PhAST in HSN and VC in animals expressing TeTx in both neurons. Note the absence of vm2 activity cannot be rescued in this condition

5.5 Inhibitory Synaptic Transmission

The construction of neuronal networks is based on a fine balance between the excitatory and inhibitory circuits. The bipartite nature of PhAST, composed of color-matched photon emitters and photosensors, affords a modular design that combines luciferases and ion channels with differing functionalities. Similar to different

neurotransmitters, luciferases that emit in different windows of the spectrum can be paired with their "cognate" channelrhodopsin that absorbs within this spectral range. For example, anion channelrhodopsins (ACRs) that conduct chloride have recently been used to efficiently silence neuronal activity [49]. ACR1 from *Guillardia theta*, among the most powerful light-gated ion channels, has an absorption maximum at 520 nm, significantly more red-shifted than the maximum of 470 nm for the commonly used excitatory channels (Table 5.3, Ref. [44]). For optimal activation, this required a green-shifted luciferase, e.g green-enhanced Nanolantern (GeNL), a fusion of the calcium-sensitive luciferase with the green fluorescent protein mNeonGreen 16. To demonstrate the functional coupling of luciferases with other inhibitory rhodopsins, we expressed ACR1 in the AVA and AIB interneurons of wild-type *C. elegans*, together with GeNL in ASH and tested their efficacy in suppressing the nose-touch evoked reversal response [18]. Importantly, without dietary supplementation of the critical cofactors, the response of the transgenic animals expressing the complete system was wildtype. However, upon delivery of ATR and the luciferin furimazine to reconstitute photosensitivity, the animal's response to nose touch was significantly reduced, as was the neuronal activity of both interneurons secondary to the stimulus. This demonstrated the efficacy of bioluminescent activated anion channelrhodopsin in suppressing the pain response resulting from silencing of endogenous synaptic transmission in a freely behaving animal [18].

5.6 Synthetic Neuronal Connections Between Unrelated Circuits

We also sought to engineer a de novo synthetic connection by rewiring the diacetyl (DA)-sensing AWA neuron with the avoidance circuit mediated by AVA and AIB. DA, a volatile attractant, activates AWA and normally suppresses reversal behavior through AIA interneurons [50]. To repolarize this attraction into an aversive response, we aimed to functionally link AWA to AVA using PhAST. While AWA and AVA lack direct synaptic connections, their axons run in parallel within the nerve ring (Fig. 5.5a).

To that end, we repurposed the AIB/AVA::ChR2-HRDC line and expressed TeNL specifically in AWA (Fig. 5.5a). To assess the behavioral relevance of these neuronal responses, we examined the ability of transgenic animals to navigate diacetyl (DA) gradients in a chemotaxis assay. In this assay, the behavioral test arena was divided into four quadrants, two of which contained DA and the other two a mock solution [51]. Importantly, PhAST transgenic animals displayed chemotaxis toward DA that was indistinguishable from wild-type (N2) animals (Fig. 5.5b, [18]), regardless of whether they received ATR or HIK alone, while odr-7 mutants that cannot sense DA failed to properly chemotax in these arenas (Fig. 5.5c). Notably, when both cofactors, HIK and ATR, were administered, the transgenic PhAST

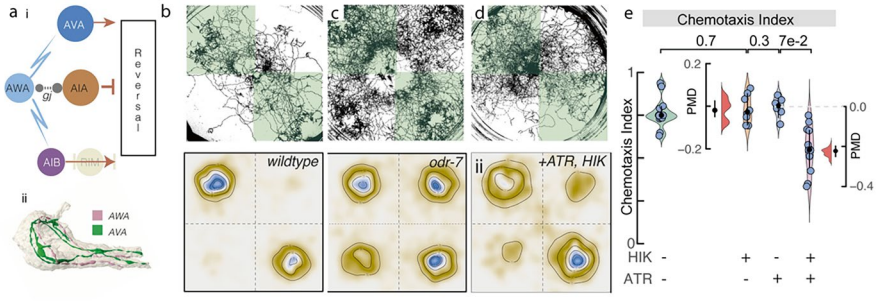

Fig. 5.5 Olfactory confusion experiment through competition between attractive and avoidance circuit. (**a**) (*i*) Sketch of the attractive AWA olfactory circuit. gj: gap junctions. Blue flashes indicate intended PhAST connections. (*ii*) 3D rendering showing the location of AWA and AVA as reconstructions from EM datasets [52]. (**b–d**) Top row: Outcome of a representative olfactory confusion experiment. Maximum intensity projections of a 30 min video recording showing the crawling trajectories of (**b**) wild type, (**c**) *odr-7*, and (**d**) PhAST animals on diacetyl-containing plates (applied on the green quadrant). Wild-type animals crawl efficiently toward the DA source, whereas *odr-7* cannot distinguish the odorant. PhAST animals are confused and do not chemotax efficiently toward the odorant. PhAST animals are confused and do not chemotax efficiently toward the odorant. Bottom row: 2D probability density function (PDF) of the animal distribution on agar plates for wild-type**,** *odr-7* mutant and PhAST transgenics, where DA was administered on the top-left and bottom-right quadrants. (**e**) Distribution of the CI for independent chemotaxis experiments, indicated as individual dots. p-value displayed above the brackets from two-sided KS test. The floating axes indicate the bootstrapped distribution of the paired median difference (PMD) between Hikarazine and ATR single-treated animals (left) and ATR single and double treated animals (right)

animals exhibited chemotaxis behavior similar to that of odr-7 mutants, as evidenced by progressively random movement resulting in less animals successfully navigating toward the DA sources (see statistics in Fig. 5.5d) and a globally reduced chemotaxis index (Fig. 5.5e). Together, this indicates that PhAST can be used to successfully connect neighboring but otherwise unconnected neurons functionally together.

5.7 Color Tuning: PhASTg and PhASTr

To fully reengineer the connectome, it would be desirable to repurpose different luciferases that emit photons with spectrally separable wavelengths and that are color-matched to specific channelrhodopsins, e.g., in the green- or red-shifted spectrum (PhASTg, PhASTr, respectively). In our previous work, we applied the cyan luciferase TeNL with an mTurquoise emitter, a green-emitting luciferase with an mNeonGreen emitter (see also Sect. 5.5 above), and an orange-emitting luciferase with the long Stokes shift cyOFP (CaMBI) [17]. Whereas cyan and green luciferases were able to noticeably trigger their cognate channelrhodopsin, CaMBI was

unable to elicit a statistically significant response with the red-shifted pump-like channelrhodopsin ChRmine [18]. The lack of signaling may be due to the relatively low operational light sensitivity of ChRmine compared to ChR2-HRDC and ACR1 (Table 5.3). However, the low bioluminescent energy transfer efficiency between the luciferase and fluorescent proteins in CaMBI likely results in an additional caveat in the insufficient photon output, which may underlie the absence of detectable signaling. Indeed, using an optimized CaMBI3 luciferase improved the PhAST results in the classical nose touch assay [27]. Thus, the field is poised to combine different luciferases to bottom-up engineer new functions and feedback loops that rely on nuanced excitatory and inhibitory input into existing structural connectomes. Unfortunately, a caveat of this approach is the broad emission spectrum of luciferases and the wide absorption range of rhodopsins, which increases the risk of spectral cross talk between different color channels. Thus, multiplexing different spectral pairs in the same circuit, especially when the wiring is compact and the targets are close together, may require the development of narrow-band emitters and sensors [53].

5.8 Summary

PhAST (photon-assisted synaptic transmission) is a synaptic engineering approach designed to replace chemical neurotransmission to create light-based connections, enabling precise information exchange between neurons within neural circuits. Unlike traditional optogenetic methods that target individual neurons, PhAST enables cell-specific directional communication by coupling presynaptic light emission to postsynaptic light sensing.

The core of the PhAST system involves engineering two separate neuronal populations: one expressing a luciferase enzyme (such as NanoLuc) and the other expressing a light-sensitive ion channel or pump, such as channelrhodopsin or ChRmine. Upon application of a luciferin substrate and the necessary cofactors, the luciferase in the presynaptic neuron emits bioluminescent photons. These photons, in turn, activate the opsin in the postsynaptic neuron, triggering a physiological response. This photon-mediated activation mimics synaptic transmission but is entirely synthetic and programmable.

Crucially, PhAST does not depend on the presence of natural synaptic contacts between paired neurons, allowing researchers to rewire circuits and create novel pathways that do not exist in the native connectome. By spatially restricting luciferase and opsin expression, PhAST enables highly specific and temporally precise modulation of activity between defined cell types, even in freely behaving animals.

This strategy has been successfully applied in *C. elegans* to several problems, including sensitization and desensitization of endogenous circuits and the conversion of an attractive cue into an aversive response in the absence of direct synaptic specializations. This flexibility makes PhAST a powerful tool for dissecting the logic of neural circuits, testing hypotheses about connectivity, and exploring how

reconfigured communication between neurons alters behavior. Looking ahead, PhAST offers a promising platform for building programmable neural networks in vitro and in vivo, enabling the design of custom information processing pathways for both basic neuroscience and therapeutic applications.

References

1. Cook SJ, Jarrell TA, Brittin CA, Wang Y, Bloniarz AE, Yakovlev MA, et al. Whole-animal connectomes of both Caenorhabditis elegans sexes. Nature. 2019;571:63–71.
2. Ripoll-Sánchez L, Watteyne J, Sun HS, Fernandez R, Taylor SR, Weinreb A, et al. The neuropeptidergic connectome of *C. elegans*. Neuron. 2023;11(111):3570–89.e5.
3. Dorkenwald S, Matsliah A, Sterling AR, Schlegel P, Chieh Yu S, McKellar CE, et al. Neuronal wiring diagram of an adult brain. Nature. 2024;10(634):124–38.
4. Bae JA, Baptiste M, Baptiste MR, Bishop CA, Bodor AL, Brittain D, et al. Functional connectomics spanning multiple areas of mouse visual cortex. Nature. 2025;4(640):435–47.
5. Chen R, Canales A, Anikeeva P. Neural recording and modulation technologies. Nat Rev Mater. 2017;1:2.
6. Emiliani V, Entcheva E, Hedrich R, Hegemann P, Konrad KR, Lüscher C, et al. Optogenetics for light control of biological systems. Nat Rev Methods Primers. 2022;2:55.
7. Aravanis AM, Wang LP, Zhang FA, Meltzer L, Mogri MZ, Schneider MB, et al. An optical neural interface: in vivo control of rodent motor cortex with integrated fiberoptic and optogenetic technology. J Neural Eng. 2007;4:S143–56.
8. Rabinowitch I, Colón-Ramos DA, Krieg M. Understanding neural circuit function through synaptic engineering. Nat Rev Neurosci. 2024;2(25):131–9.
9. Chen R, Gore F, Nguyen QA, Ramakrishnan C, Patel S, Kim SH, et al. Deep brain optogenetics without intracranial surgery. Nat Biotechnology. 2021;39:161–4.
10. Alekseev, A., Hunniford, V., Zerche, M. et al. Efficient and sustained optogenetic control of sensory and cardiac systems. Nat. Biomed. Eng (2025). https://doi.org/10.1038/s41551-025-01461-1
11. Gong X, Mendoza-Halliday D, Ting JT, Kaiser T, Sun X, Bastos AM, et al. An ultra-sensitive step- function opsin for minimally invasive optogenetic stimulation in mice and macaques. Neuron. 2020;107:38–51.e8.
12. Porta-de-la Riva M, Morales-Curiel LF, Gonzalez A, Krieg M. Bioluminescence as a functional tool for visualizing and controlling neuronal activity in vivo. Neurophotonics. 2024;11:1–26.
13. Wang W, Wu X, Tang KWK, Pyatnitskiy I, Taniguchi R, Lin P, et al. Ultrasound-triggered in situ photon emission for noninvasive optogenetics. J Am Chem Soc. 2023;145:1097–107.
14. Wu X, Zhu X, Chong P, Liu J, Andre LN, Ong KS, et al. Sono-optogenetics facilitated by a circulationdelivered rechargeable light source for minimally invasive optogenetics. Proc Natl Acad Sci U S A. 2019;116:26332–42.
15. Matsubara T, Yanagida T, Kawaguchi N, Nakano T, Yoshimoto J, Sezaki M, et al. Remote control of neural function by X-ray-induced scintillation. Nat Commun. 2021:12.
16. Suzuki K, Kimura T, Shinoda H, Bai G, Daniels MJ, Arai Y, et al. Five colour variants of bright luminescent protein for real-time multicolour bioimaging. Nat Commun. 2016;7:1–10.
17. Oh Y, Park Y, Cho JH, Wu H, Paulk NK, Liu LX, et al. An orange calcium-modulated bioluminescent indicator for non-invasive activity imaging. Nat Chem Biol. 2019;15:433–6.
18. Porta-de-la Riva M, Gonzalez AC, Sanfeliu-Cerdán N, Karimi S, Malaiwong N, Pidde A, et al. Neural engineering with photons as synaptic transmitters. Nat Methods. 2023;20:761–9.
19. Mirdita M, Schütze K, Moriwaki Y, Heo L, Ovchinnikov S, Steinegger M. ColabFold: making protein folding accessible to all. Nat Methods. 2022;6(19):679–82.

20. Piggott BJ, Liu J, Feng Z, Wescott SA, Xu XZS. The neural circuits and synaptic mechanisms underlying motor initiation in *C. elegans*. Cell. 2011;147:922–33.
21. Takai A, Nakano M, Saito K, Haruno R, Watanabe TM, Ohyanagi T, et al. Expanded palette of nano-lanterns for real-time multicolor luminescence imaging. Proc Natl Acad Sci U S A. 2015;112:4352–6.
22. Morales-Curiel LF, Gonzalez AC, Castro-Olvera G, Lin LCL, El-Quessny M, Porta-de-la Riva M, et al. Volumetric imaging of fast cellular dynamics with deep learning enhanced bioluminescence microscopy. Commun Biol. 2022;5:1330.
23. Farhana I, Hossain MN, Suzuki K, Matsuda T, Nagai T. Genetically encoded fluorescence/bioluminescence bimodal indicators for Ca2+ imaging. ACS Sens. 2019;4:1825–34.
24. Qian Y, Rancic V, Wu J, Ballanyi K, Campbell RE. A bioluminescent Ca 2+ indicator based on a topological variant of GCaMP6s. ChemBioChem. 2019;20:516–20.
25. Tian X, Zhang Y, Li X, Xiong Y, Wu T, Ai HW. A luciferase prosubstrate and a red bioluminescent calcium indicator for imaging neuronal activity in mice. Nat Commun. 2022:13.
26. Lambert GG, Crespo EL, Murphy J, Boassa D, Luong S, Celinskis D, et al. CaBLAM: A high-contrast bioluminescent Ca2+ indicator derived from an engineered Oplophorus gracilirostris luciferase. Nature Methods. 2026;23:205–15.
27. Zhao Y, Lee S, Campbell RE, Lin MZ. Directed evolution of a genetically encoded bioluminescent Ca2+ Sensor. Eng Proc. 2023;35:20.
28. Petersen ED, Lapan AP, Fillion AJ, Crespo EL, Lambert GG, Zanca AT, et al. Bioluminescent genetically encoded glutamate indicator for molecular imaging of neuronal activity. ACS Synth Biol. 2023;12:2301–9.
29. Erdenee E, Ting AY. A dual-purpose real-time indicator and transcriptional integrator for calcium detection in living cells. ACS Synth Biol. 2022;3(11):1086–95.
30. Yoshida T, Kakizuka A, Imamura H. BTeam, a novel BRET-based biosensor for the accurate quantification of ATP concentration within living cells. Sci Rep. 2016;12:6.
31. Gregor C, Pape JK, Gwosch KC, Gilat T, Sahl SJ, Hell SW. Autonomous bioluminescence imaging of single mammalian cells with the bacterial bioluminescence system. Proc Natl Acad Sci U S A. 2019;116:26491–6.
32. Tanaka R, Sugiura K, Osabe K, Hattori M, Nagai T. Genetically encoded bioluminescent glucose indicator for biological research. Biochem Biophys Res Commun. 2025;1:742.
33. Yeh HW, Ai HW. Development and applications of bioluminescent and chemiluminescent reporters and biosensors. Annu Rev Anal Chem. 2019;12:129–50.
34. Syed AJ, Anderson JC. Applications of bioluminescence in biotechnology and beyond. Chem Soc Rev. 2021;50:5668–705.
35. Dijkema FM, Nordentoft MK, Didriksen AK, Corneliussen AS, Willemoës M, Winther JR. Flash properties of Gaussia luciferase are the result of covalent inhibition after a limited number of cycles. Prot Sci. 2021;30:638–49.
36. Yeh HW, Xiong Y, Wu T, Chen M, Ji A, Li X, et al. ATP-independent bioluminescent reporter variants to improve in vivo imaging. ACS Chem Biol. 2019;14:959–65.
37. Nagel G, Szellas T, Huhn W, Kateriya S, Adeishvili N, Berthold P, et al. Channelrhodopsin-2, a directly light-gated cation-selective membrane channel. Proc Natl Acad Sci. 2003;100:13940–5.
38. Nagel G, Brauner M, Liewald JF, Adeishvili N, Bamberg E, Gottschalk A. Light activation of Channelrhodopsin-2 in excitable cells of caenorhabditis elegans triggers rapid behavioral responses. Curr Biol. 2005;15:2279–84.
39. Dawydow A, Gueta R, Ljaschenko D, Ullrich S, Hermann M, Ehmann N, et al. Channelrhodopsin-2- XXL, a powerful optogenetic tool for low-light applications. Proc Natl Acad Sci. 2014;111:13972–7.
40. Bergs A, Schultheis C, Fischer E, Tsunoda SP, Erbguth K, Husson SJ, et al. Rhodopsin optogenetic toolbox v2.0 for light-sensitive excitation and inhibition in Caenorhabditis elegans. PLoS One. 2018;13:1–24.

41. Govorunova EG, Gou Y, Sineshchekov OA, Li H, Lu X, Wang Y, et al. Kalium channelrhodopsins are natural light-gated potassium channels that mediate optogenetic inhibition. Nat NeuroScience. 2022;7(25):967–74.
42. Morizumi T, Kim K, Li H, Nag P, Dogon T, Sineshchekov OA, et al. Structural insights into lightgating of potassium-selective channelrhodopsin. Nat Commun. 2025;12(16):1283.
43. Sineshchekov OA, Govorunova EG, Li H, Wang Y, Melkonian M, Wong GKS, et al. Conductance mechanisms of rapidly desensitizing cation channelrhodopsins from cryptophyte algae. mBio. 2020;11.
44. Govorunova EG, Sineshchekov OA, Janz R, Liu X, Spudich JL. Natural light-gated anion channels: a family of microbial rhodopsins for advanced optogenetics. Science (New York, NY). 2015;349:647–50.
45. Durduran T, Zhou C, Edlow BL, Yu G, Choe R, Kim MN, et al. Transcranial optical monitoring of cerebrovascular hemodynamics in acute stroke patients. Opt Exp. 2009;17:3884.
46. Pechuk V, Goldman G, Salzberg Y, Chaubey AH, Bola RA, Hoffman JR, et al. Reprogramming the topology of the nociceptive circuit in *C. elegans* reshapes sexual behavior. Curr Biol. 2022;32:4372–85.e7.
47. Schafer WR. Egg-laying. WormBook: the online review of C elegans biology. 2005:1–7.
48. Collins KM, Bode A, Fernandez RW, Tanis JE, Brewer JC, Creamer MS, et al. Activity of the *C. elegans* egg-laying behavior circuit is controlled by competing activation and feedback inhibition. eLife. 2016;5:1–24.
49. Mahn M, Gibor L, Patil P, Malina KCK, Oring S, Printz Y, et al. High-efficiency optogenetic silencing with soma-targeted anion-conducting channelrhodopsins. Nat Commun. 2018;12:9.
50. Larsch J, Flavell SW, Liu Q, Gordus A, Albrecht DR, Bargmann CI. A circuit for gradient climbing in *C. elegans* chemotaxis. Cell Rep. 2015;12:1748–60.
51. Margie O, Palmer C, Chin-Sang I. *C. elegans* chemotaxis assay. J Vis Exp. 2013:1–6.
52. Witvliet D, Mulcahy B, Mitchell JK, Meirovitch Y, Berger DR, Wu Y, et al. Connectomes across development reveal principles of brain maturation. Nature. 2021;596:257–61.
53. Carrasco-López C, Lui NM, Schramm S, Naumov P. The elusive relationship between structure and colour emission in beetle luciferases. Nat Rev Chem. 2021;5:4–20.